symmetry

MDPI

Article

Analytical Methods for Fractional Differential Equations: Time-Fractional Foam Drainage and Fisher's Equations

Abdulrahman B. M. Alzahrani [1,*] and Ghadah Alhawael [2]

[1] Department of Mathematics, College of Science, King Saud University, P.O. Box 2455, Riyadh 11451, Saudi Arabia
[2] Department of Basic Sciences, Common First Year Deanship, King Saud University, P.O. Box 145111, Riyadh 11362, Saudi Arabia; galhawil@ksu.edu.sa
* Correspondence: aalzahranii@ksu.edu.sa

Abstract: In this research, we employ a dual-approach that combines the Laplace residual power series method and the novel iteration method in conjunction with the Caputo operator. Our primary objective is to address the solution of two distinct, yet intricate partial differential equations: the Foam Drainage Equation and the nonlinear time-fractional Fisher's equation. These equations, essential for modeling intricate processes, present analytical challenges due to their fractional derivatives and nonlinear characteristics. By amalgamating these distinctive methodologies, we derive precise and efficient solutions substantiated by comprehensive figures and tables showcasing the accuracy and reliability of our approach. Our study not only elucidates solutions to these equations, but also underscores the effectiveness of the Laplace Residual Power Series Method and the New Iteration Method as potent tools for grappling with intricate mathematical and physical models, thereby making significant contributions to advancements in diverse scientific domains.

Keywords: Foam Drainage Equation; nonlinear time-fractional Fisher's equation; Laplace Residual Power Series Method; New Iteration Method; Caputo operator; fractional-order differential equation

Citation: Alzahrani, A.B.M.; Alhawael, G. Analytical Methods for Fractional Differential Equations: Time-Fractional Foam Drainage and Fisher's Equations. *Symmetry* **2023**, *15*, 1939. https://doi.org/10.3390/sym15101939

Academic Editors: Muhammad I. Syam, Abdul-Majid Wazwaz, Mohammed Al-Refai and Junesang Choi

Received: 2 September 2023
Revised: 11 October 2023
Accepted: 16 October 2023
Published: 19 October 2023

1. Introduction

Ordinary and partial fractional-order differential equations have gotten much attention because they are often used in fields like fluid mechanics, biology, physics, and engineering. As a result, a great deal of work has gone into finding answers to physical-world fractional ordinary differential equations, integral equations, and fractional partial differential equations [1–8]. To characterize a broad range of nonlinear physical and natural processes, fractional partial differential equations (FPDEs) have been presented to play a crucial role [9–11]. Despite its importance, solving such equations is difficult, leading to investigating various numerical techniques that may provide approximations. Recent articles [12–21] and their corresponding references are recommended reading for anybody interested in learning more.

Fractional-order differential equations are of great importance in the study of physical processes. Throughout time, several analytical and numerical approaches have been developed to tackle the difficulties they present. The Adomian decomposition method [13–16], the variational iteration method [13], the fractional difference method [6], the differential transform method [22], and the homotopy perturbation method [23] are particularly noteworthy examples of such approaches. The Laplace transform, fractional Green's function, Mellin transform, and orthogonal polynomial techniques are only a few of the traditional solution approaches that are relevant here [6]. Together, these techniques provide a rich tool for addressing the complex problems posed by fractional differential equations in many fields of study [24–26].

Symmetry plays a pivotal role in the analysis of fractional differential equations, offering a powerful lens through which complex mathematical models can be understood and solved. Fractional-order symmetries, akin to their counterparts in traditional differential equations, provide a means to reduce problem dimensionality and unveil common solution properties. Utilizing Lie group theory and symmetry reduction techniques, researchers can identify invariant solutions, classify equations, and gain deeper insights into the underlying principles governing diverse phenomena in fields such as fluid dynamics, heat conduction, and population dynamics. This interdisciplinary approach not only simplifies the study of fractional differential equations, but also unveils the fundamental symmetries that underlie the behavior of physical systems, bridging the realms of mathematics and physics to yield valuable insights and discoveries.

The nonlinear time-fractional Foam Drainage Equation is of the form

$$D_{\delta}^{p}\xi = \frac{1}{2}\xi\xi_{\gamma\gamma} - 2\xi^2\xi_{\gamma} + \xi_{\gamma}^2, \delta > 0,$$

associated with the initial condition $\xi(\gamma, 0) = f(\gamma)$, where $\xi := \xi(\gamma, \delta)$ and $0 < \delta \leq 1$. Here, γ represents the scaled position coordinate, δ represents the time, and ξ is the plateau border cross-sectional area. Foams, whether liquid or solid, have a wide range of industrial [27] and every day [28] uses for scientists and the general public. In order to stabilize the liquid–gas interfaces, bubbles are infused into a liquid containing a surfactant. Underground fluid flow in cracked and porous media exhibits a variety of hydromechanical phenomena that have piqued researchers' curiosity for decades. Foaming happens in a variety of absorption and distillation processes. Foam is a great example of a multi-phase "soft condensed matter" system in foam drainage [29]. Foams frequently have a convoluted, chaotic structure, with the components being liquid sheets that meet plateau limits. As the cross-sections of plateau boundaries grow, more liquid is integrated into the foam. The drainage model has several uses, including commodity care such as lotions, oils, creams, and textile washing [30], structural material sciences, mineral processing, chemical industries [31], and aluminum metals [32]. During the creation of foams, the material is in a liquid state, and the fluid might change while the bubble structure remains roughly the same. They are also found in lightweight mechanical components, acoustic cladding, heat exchangers, impact-absorbing portions on automobiles, and textured wallpapers, where they are used as foamy inks. Foams are significant in many technical applications and processes, and their properties are of interest from both a practical and scientific standpoint.

Fisher proposed Fisher's equation [33] in 1937 as a model for the temporal and geographical propagation of a virile gene in an infinite media. The reaction–diffusion equation is the simplest and most-traditional instance of Fisher's equation [34]:

$$\frac{\partial\xi}{\partial\delta} = \lambda\frac{\partial^2\xi}{\partial\gamma^2} + \mu\xi(\gamma, \delta)(1 - \xi(\gamma, \delta)),$$

It is essentially the Logistic equation and the combination of the diffusion equation with the diffusion factor λ and the birth rate μ. In this case, $\xi(\gamma, \delta)$ describes the state development throughout the spatial–temporal domain defined by the coordinates γ, δ. Fisher's equation is widely applied in Neolithic transitions [35], chemical kinetics [36], epidemics and bacteria [37], branching Brownian motion [38], and many other disciplines.

The Laplace transform, named after Pierre-Simon Laplace, is a sophisticated mathematical tool utilized in various subjects, including engineering, physics, and mathematics. It transforms time functions into complex variable functions, making studying linear time-invariant systems and solving complex differential equations easier [39,40]. The Laplace transform facilitates problem solving by translating complex equations into simpler algebraic forms. It also gives insights into the frequency and decay features of functions. The Laplace transform is a key tool that increases our knowledge of dynamic systems and allows developments in different scientific and technical disciplines. It is widely used in circuit analysis, control systems, signal processing, and beyond [41,42].

The Laplace Residual Power Series Method is a sophisticated mathematical approach for solving ODEs with variable coefficients. This methodology, which was built based on the Laplace transform and power series approaches, leverages its strengths to handle a class of ODEs that are difficult to solve using standard techniques. The approach provides a systematic methodology to estimate solutions for complex and nonlinear differential equations by translating the differential equation into a Laplace-transformed form and, then, expanding the resultant expression into a power series. The Laplace Residual Power Series Method extends the reach of problem-solving capabilities, particularly in cases where direct analytical solutions are elusive, allowing researchers and practitioners to gain deeper insights into a wide range of dynamic systems across diverse fields [43–47].

Developing a new iterative approach for fractional partial differential equations represents a significant step forward in mathematical analysis and problem solving. Traditional approaches frequently face computational complexity and convergence issues when solving partial differential equations with fractional derivatives. This unique iterative strategy tries to overcome these restrictions by iteratively refining approximation solutions, gradually improving accuracy while retaining the computing economy. This technique can provide superior solutions for a wide range of complicated mathematical and physical phenomena by leveraging the power of iteration and customizing it to the particular properties of fractional derivatives [48–50]. Its advent opens the door to solving challenging issues in physics, engineering, and applied mathematics, improving our capacity to model and comprehend complex systems governed by fractional partial differential equations.

The Laplace Residual Power Series Method (LRPSM) [43–46] and the New Iteration Method (NIM) [48–50] are the most-straightforward ways to solve fractional differential equations because they give immediate and visible symbolic terms of analytic solutions, as well as numerically approximate solutions to both linear and nonlinear differential equations without linearization or discretization. The main goal of this work is to find the solutions to two nonlinear partial differential equations, the Foam Drainage Equation and the nonlinear time-fractional Fisher's equation, using two different methods, LRPSM and NIM, and compare how well they work. We need to bring to the reader's attention to the fact that these two methods have been used to solve several different types of nonlinear fractional differential problems.

The outline of this paper is as follows. In Section 2, we begin by providing some basic definitions that are used in our study. The road map of the proposed methods (LRPSM and NIM) is illustrated in Section 3. The implementation of the proposed methods and the discussion of the results are presented in Section 4. Finally, Section 5 includes the conclusions of our study.

2. Basic Definitions

Definition 1. *For $p \in \mathbb{R}^+$, the Riemann–Liouville fractional integral operator for p real-valued function $\sim(\gamma, \delta)$ is denoted by $\mathcal{J}_\delta^p$ and defined as [51]:*

$$\mathcal{J}_\delta^p \xi(\gamma,\delta) = \begin{cases} \frac{1}{\Gamma(p)} \int_0^\delta \frac{\xi(\gamma,\eta)}{(\delta-\eta)^{1-p}} d\eta, & 0 \le \eta < \delta, p > 0 \\ \sim(\gamma,\delta), & p = 0. \end{cases}$$

Definition 2. *The time-fractional derivative of order $p > 0$, for the function $\xi(\gamma,\delta)$ in the Caputo case, is denoted by D_δ^p and defined as [51]:*

$$D_\delta^p \xi(\gamma,\delta) = \begin{cases} \mathfrak{J}_\delta^{n-p}\left(D_\delta^n \xi(\gamma,\delta)\right), & 0 < n-1 < p \le n, \\ D_\delta^n \xi(\gamma,\delta)), & p = n, \end{cases}$$

where $D_\delta^n = \frac{\partial^n}{\partial \delta^n}$ and $n \in \mathbb{N}$.

Consequently, for $n-1 < p \le n, \beta > -1$ and $\delta \ge 0$, the operators D_δ^p and $\mathfrak{J}_\delta^p$ satisfy the following properties:

1. $D^{p}_{\delta}c = 0, c \in \mathbb{R}$.
2. $D^{p}_{\delta}\delta^{\beta} = \frac{\Gamma(\beta+1)}{\Gamma(\beta+1-p)}\delta^{\beta-p}$.
3. $D^{p}_{\delta}\mathfrak{J}^{p}_{\delta}\xi(\gamma,\delta) = \xi(\gamma,\delta)$.
4. $\mathfrak{J}^{p}_{\delta}D^{p}_{\delta}\xi(\gamma,\delta) = \xi(\gamma,\delta) - \sum_{j=0}^{n-1} D^{j}_{\delta}(\gamma,0^{+})\frac{\delta^{j}}{j!}$, *for* $\xi \in C^{n}[a,b], n-1 < p \leq n, n \in \mathbb{N}$ *and* $a,b \in \mathbb{R}$.

Definition 3. *Let $\xi(\gamma,\delta)$ be a piecewise continuous function on $I \times [0,\infty)$ and of exponential order ϱ. Then, the Laplace transformation of the function $\xi(\gamma,\delta)$ is denoted and defined as follows [51]:*

$$\xi(\gamma,s) = \mathcal{L}[\xi(\gamma,\delta)] := \int_{0}^{\infty} e^{-s\delta}\xi(\gamma,\delta)d\delta, \ \ s > \varrho,$$

whereas the inverse Laplace transformation of the function $\xi(\gamma,s)$ is defined as follows:

$$\xi(\gamma,\delta) = \mathcal{L}^{-1}[\xi(\gamma,s)] := \frac{1}{2\pi i}\int_{c-i\infty}^{c+i\infty} e^{s\delta}\xi(\gamma,s)ds, \quad c = \mathrm{Re}(s) > \varrho_{0},$$

where ϱ_0 lies in the right half-plane of the absolute convergence of the Laplace integral.

3. Road Map of the Proposed Methods

3.1. General Procedure of the Laplace Residual Power Series Method

Consider the partial differential equation of fractional order:

$$\begin{aligned} D^{p}_{\delta}\xi(\gamma,\delta) &= N_{\gamma}[\xi(\gamma,\delta)] \\ \xi(\gamma,0) &= f(\gamma) \end{aligned} \tag{1}$$

where N_{γ} is a nonlinear operator relative to γ of degree $r, \gamma \in I, \delta \geq 0, D^{p}_{\delta}$ refers to the pth Caputo fractional derivative for $p \in (0,1]$, and $\xi(\gamma,\delta)$ is an unknown function to be determined.

To construct the approximate solution of (1) by using the Laplace RPSM, one can perform the following procedure:

Step 1: Apply the Laplace transform on both sides of (1) and utilize the initial data of (1):

$$\begin{aligned} \varpi(\gamma,s) = \frac{f(x)}{s} - \frac{1}{s^{a}}\mathcal{L}\{N_{\gamma}[\xi(\gamma,\delta)]\}, \\ \text{where } \varpi(\gamma,s) = \mathcal{L}[\xi(\gamma,\delta)](s), s > \delta. \end{aligned} \tag{2}$$

Step 2: We assume that the approximate solution of the Laplace Equation (2) takes the following fractional expansion:

$$\varpi(\gamma,s) = \frac{f(x)}{s} + \sum_{n=1}^{\infty}\frac{h_{n}(x)}{s^{np+1}}, x \in I, s > \delta \geq 0, \tag{3}$$

and the kth Laplace series solution takes the following form:

$$\varpi_{k}(\gamma,s) = \frac{f(x)}{s} + \sum_{n=1}^{k}\frac{h_{n}(x)}{s^{n}p+1}, \gamma \in I, s > \delta \geq 0. \tag{4}$$

Step 3: We define the kth Laplace fractional residual function of (2) as

$$\mathcal{L}\big(\mathrm{Res}_{\varpi_{k}}(\gamma,s)\big) = \varpi_{k}(\gamma,s) - \frac{f(x)}{s} + \frac{1}{s}\mathcal{L}\{N_{\gamma}[\xi(\gamma,\delta)]\}, \tag{5}$$

and the Laplace residual function of (2) is defined as:

$$\lim_{k\to\infty}\mathcal{L}\big(\mathrm{Res}_{\varpi_k}(\gamma,s)\big)=\mathcal{L}(\mathrm{Res}_{\varpi}(\gamma,s))=\varpi(\gamma,s)-\frac{f(x)}{s}+\frac{1}{s^p}\mathcal{L}\{N_\gamma[\xi(\gamma,\delta)]\}. \tag{6}$$

Some useful facts of the Laplace residual function that are essential in finding the approximate solution are listed as follows: $-\lim_{k\to\infty}\mathcal{L}\big(\mathrm{Res}_{\varpi_k}(\gamma,s)\big)=\mathcal{L}(\mathrm{Res}_{\varpi}(\gamma,s))$, for $\gamma\in I, s>\delta\geq 0$. $-\mathcal{L}(\mathrm{Res}_{\varpi}(\gamma,s))=0$, for $\gamma\in I, s>\delta\geq 0$. $-\quad \lim_{s\to\infty}s^{kp+1}\mathcal{L}\big(\mathrm{Res}_{\varpi_k}(\gamma,s)\big)=0$, for $\gamma\in I, s>\delta\geq 0$, and $k=1,2,3,\ldots$

Step 4: Substitute the kth Laplace series solution (4) into the kth Laplace fractional residual function of (5).

Step 5: The unknown coefficients $h_k(x)$, for $k=1,2,3,\ldots$, could be founded by solving the system $\lim_{s\to\infty}s^{ka+1}\mathcal{L}\big(\mathrm{Res}_{\varpi_k}(\gamma,s)\big)=0$. Then, we collect the obtained coefficients in terms of fractional expansion series (4) $\varpi_k(\gamma,s)$.

Step 6: Run the inverse Laplace transform operator on both sides of the obtained Laplace series solution to get the approximate solution $\xi_k(\gamma,\delta)$, of the main Equation (1).

3.2. Basic Idea of New Iterative Method

Here, we present some basic steps for deriving the new iterative method [52]. Assume the nonlinear equation:

$$\xi(\gamma,\delta)=f(\gamma,\delta)+M\xi(\gamma,\delta)+N\kappa(\gamma,\delta), \tag{7}$$

where g is a known function, M denotes the linear operator, and N denotes the nonlinear operator from a Banach space B $\to$ B. According to NIM, the solution of the above Equation (7) can be expanded as:

$$\xi(\gamma,\delta)=\sum_{m=0}^{\infty}\xi_m(\gamma,\delta), \tag{8}$$

due to the linearity of the M operator:

$$M\left(\sum_{m=0}^{\infty}\xi_m(\gamma,\delta)\right)=\sum_{m=0}^{\infty}M(\xi_m(\gamma,\delta)), \tag{9}$$

N is nonlinear and can be expanded as

$$N\left(\sum_{m=0}^{\infty}\xi_m(\gamma,\delta)\right)=N(\xi_0(\gamma,\delta))+\sum_{m=1}^{\infty}\left\{N\left(\sum_{j=0}^{m}\xi_j(\gamma,\delta)\right)-N\left(\sum_{j=0}^{m-1}\xi_j(\gamma,\delta)\right)\right\}, \tag{10}$$

and by the use of Equations (8)–(10), the general Equation (7) takes the form

$$\sum_{i=1}^{\infty}\xi_i=f+\sum_{m=0}^{\infty}M(\xi_m)+N(\xi_0)+\sum_{m=1}^{\infty}\left[N\left(\sum_{j=0}^{m}\xi_j\right)-N\left(\sum_{j=0}^{m-1}\xi_j\right)\right]; \tag{11}$$

to obtain the solution components, the recursive relation can be defined as

$$\begin{cases}\xi_0(\gamma,\delta)=f\\ \xi_1(\gamma,\delta)=M(\xi_0)+N(\xi_0)\\ \xi_2(\gamma,\delta)=M(\xi_1)+N(\xi_0+\xi_1)-N(\xi_0)\\ \vdots\\ \xi_m(\gamma,\delta)=M(\xi_{m-1})+N(\xi_0+\xi_1+\ldots+\xi_{m-1})-N(\xi_0+\xi_1+\ldots+\xi_{m-2}).\end{cases}$$

The m-terms that approximate the solution of Equations (7) and (8) are given as

$$\xi(\gamma,\delta)=\xi_o+\xi_1+\ldots+\xi_{m-1}. \tag{12}$$

3.3. Convergence of New Iterative Method Theorem

If $\aleph$ is analytic in a neighborhood of ξ_0 and

$$\|N'''(\xi_0)\| = \sup\{N^m(\xi_0)(b_1, b_2, \ldots..b_n)/\|b_k\| \leq 1, 1 \leq k \leq m\} \leq l,$$

for any number m and for some real number $l > 0$ and $\|\xi_k\| \leq M < \frac{1}{e}, k = 1, 2, \ldots$, then the series $\sum_{m=0}^{\infty} G_m$ is absolutely convergent and, moreover,

$$\|G_m\| \leq lM^m e^{m-1}(e-1), m = 1, 2, \cdots$$

Now, to show boundedness of $\|\xi_k\|$, for every k, the conditions on $N^{(j)}(\xi_0)$ are given that are sufficient to guarantee the convergence of the series. The following theorem gives the sufficient conditions for the convergence of the method.

3.4. Theorem

If N is C^∞ and $\|N^m(\xi_0)\| \leq M \leq e^{-1}$ for all m, then the series $\sum_{m=0}^{\infty} G_m$ is absolutely convergent. These are the conditions of the convergence of the series $\sum_{j=0}^{\infty} \xi_j$. The proofs of the theorem can be seen in [53].

4. Numerical problems

4.1. Problem

Consider the time-fractional Fisher's equation given as

$$D_\delta^p \xi(\gamma, \delta) - \frac{\partial^2 \xi(\gamma, \delta)}{\partial \gamma^2} - 6\xi(\gamma, \delta) + 6\xi^2(\gamma, \delta) = 0, \quad \text{where} \quad 0 < p \leq 1, \tag{13}$$

subject to the following ICs:

$$\xi(\gamma, 0) = \frac{1}{(1 + e^\gamma)^2}. \tag{14}$$

The exact solution is

$$\xi(\gamma, \delta) = \frac{1}{(1 + e^{\gamma - 5\delta})^2}.$$

Implementation of Laplace Residual Power Series Method

Applying the LT to Equation (13), and making use of Equation (14), we get

$$\xi(\gamma, s) - \frac{\frac{1}{(1+e^\gamma)^2}}{s} - \frac{1}{s^p} \frac{\partial^2 \xi(\gamma, s)}{\partial \gamma^2} - \frac{6}{s^p} \xi(\gamma, s) + \frac{6}{s^p} \mathcal{L}_\delta[(\mathcal{L}_\delta^{-1}[\xi(\gamma, s)])^2] = 0, \tag{15}$$

and so, the kth truncated term series are

$$\xi(\gamma, s) = \frac{\frac{1}{(1+e^\gamma)^2}}{s} + \sum_{r=1}^{k} \frac{f_r(\gamma, s)}{s^{rp+1}}, \quad r = 1, 2, 3, 4 \cdots. \tag{16}$$

The Laplace residual functions (LRFs) [54] are

$$\mathcal{L}_\delta Res(\gamma, s) = \xi(\gamma, s) - \frac{\frac{1}{(1+e^\gamma)^2}}{s} - \frac{1}{s^p} \frac{\partial^2 \xi(\gamma, s)}{\partial \gamma^2} - \frac{6}{s^p} \xi(\gamma, s) + \frac{6}{s^p} \mathcal{L}_\delta[(\mathcal{L}_\delta^{-1}[\xi(\gamma, s)])^2] = 0, \tag{17}$$

and the kth LRFs are:

$$\mathcal{L}_\delta Res_k(\gamma,s) = \xi_k(\gamma,s) - \frac{\frac{1}{(1+e^\gamma)^2}}{s} - \frac{1}{s^p}\frac{\partial^2 \xi_k(\gamma,s)}{\partial\gamma^2} - \frac{6}{s^p}\xi_k(\gamma,s) + \frac{6}{s^p}\mathcal{L}_\delta[(\mathcal{L}_\delta^{-1}[\xi_k(\gamma,s)])^2] = 0. \tag{18}$$

Now, to determine $f_r(\gamma,s)$, $r = 1,2,3,\cdots$, we substitute the rth truncated series Equation (16) into the rth Laplace residual function Equation (18), multiply the resulting equation by s^{rp+1}, and then, recursively solve the relation $\lim_{s\to\infty}(s^{rp+1}\mathcal{L}_\delta Res_{\xi,r}(\gamma,s)) = 0$, $r = 1,2,3,\cdots$. The following are the first few terms:

$$f_1(\gamma,s) = \frac{10e^\gamma}{(1+e^\gamma)^3}, \tag{19}$$

$$f_2(\gamma,s) = \frac{50e^\gamma(-1+2e^\gamma)}{(1+e^\gamma)^4}, \tag{20}$$

and so on.

Putting the values of $f_r(\gamma,s)$, $r = 1,2,3,\cdots$, into Equation (16), we get

$$\xi(\gamma,s) = \frac{1}{s}\Big(\frac{1}{(1+e^\gamma)^2}\Big) + \frac{1}{s^{p+1}}\Big(\frac{10e^\gamma}{(1+e^\gamma)^3}\Big) + \frac{1}{s^{2p+1}}\Big(\frac{50e^\gamma(-1+2e^\gamma)}{(1+e^\gamma)^4}\Big) + \cdots. \tag{21}$$

Using the inverse Laplace transform, we get

$$\xi(\gamma,\delta) = \frac{1}{(1+e^\gamma)^2} + \frac{\delta^p}{\Gamma(p+1)}\Big(\frac{10e^\gamma}{(1+e^\gamma)^3}\Big) + \frac{\delta^{2p}}{\Gamma(2p+1)}\Big(\frac{50e^\gamma(-1+2e^\gamma)}{(1+e^\gamma)^4}\Big) + \cdots \tag{22}$$

Implementation of New Iteration Method

Applying the RL integral to Equation (13), we get the equivalent form:

$$\xi(\gamma,\delta) = \frac{1}{(1+e^\gamma)^2} - \Re_\delta^p\Big[\frac{\partial^2\xi(\gamma,\delta)}{\partial\gamma^2} + 6\xi(\gamma,\delta) - 6\xi^2(\gamma,\delta)\Big] \tag{23}$$

According to the NIM procedure, we get the following few terms:

$$\begin{aligned}
\xi_0(\gamma,\delta) &= \frac{1}{(1+e^\gamma)^2},\\
\xi_1(\gamma,\delta) &= \frac{(-3+5e^\gamma(1+e^\gamma))\delta^p}{(1+e^\gamma)^4\Gamma[1+p]},\\
\xi_2(\gamma,\delta) &= \frac{\delta^{2p}}{2(1+e^\gamma)^8}\Big(\frac{(1+e^\gamma)^2(54+e^\gamma(-109+e^\gamma(-126+25e^\gamma(3+2e^\gamma))))}{\Gamma[1+2p]}\\
&\quad - \frac{3\times 4^{p+1}(3-5e^\gamma(1+e^\gamma))^2 p^p\Gamma[\frac{1}{2}+p]}{\sqrt{\pi}\Gamma[1+p]\Gamma[1+3p]}\Big)
\end{aligned} \tag{24}$$

By the NIM algorithm, the final solution is

$$\xi(\gamma,\delta) = \xi_0(\gamma,\delta) + \xi_1(\gamma,\delta) + \xi_2(\gamma,\delta) + \cdots \tag{25}$$

$$\begin{aligned}
\xi(\gamma,\delta) =& \frac{1}{(1+e^\gamma)^2} + \frac{(-3+5e^\gamma(1+e^\gamma))\delta^p}{(1+e^\gamma)^4\Gamma[1+p]} + \frac{\delta^{2p}}{2(1+e^\gamma)^8}\Big(\frac{(1+e^\gamma)^2(54+e^\gamma(-109+e^\gamma(-126+25e^\gamma(3+2e^\gamma))))}{\Gamma[1+2p]}\\
&- \frac{3\times 4^{p+1}(3-5e^\gamma(1+e^\gamma))^2 p^p\Gamma[\frac{1}{2}+p]}{\sqrt{\pi}\Gamma[1+p]\Gamma[1+3p]}\Big) + \cdots
\end{aligned} \tag{26}$$

In Figure 1, the graphical representation highlights the effectiveness of the Laplace Residual Power Series Method (LRPSM) in solving Fisher's equation with varying fractional orders. Subplots (a)–(d) showcase the LRPSM results for fractional orders 0.7, 0.8, 0.9, and 1.0, respectively, while keeping the value of the parameter δ as 0.01. These subplots offer insights into how different fractional orders influence the behavior of the solution. Table 1 comprehensively compares the LRPSM solutions for different fractional orders in Section 4.1, with δ set to 0.01. This tabulated data offer a quantitative perspective on the impact of fractional-order variations on the accuracy and efficiency of the LRPSM approach in solving Fisher's equation.

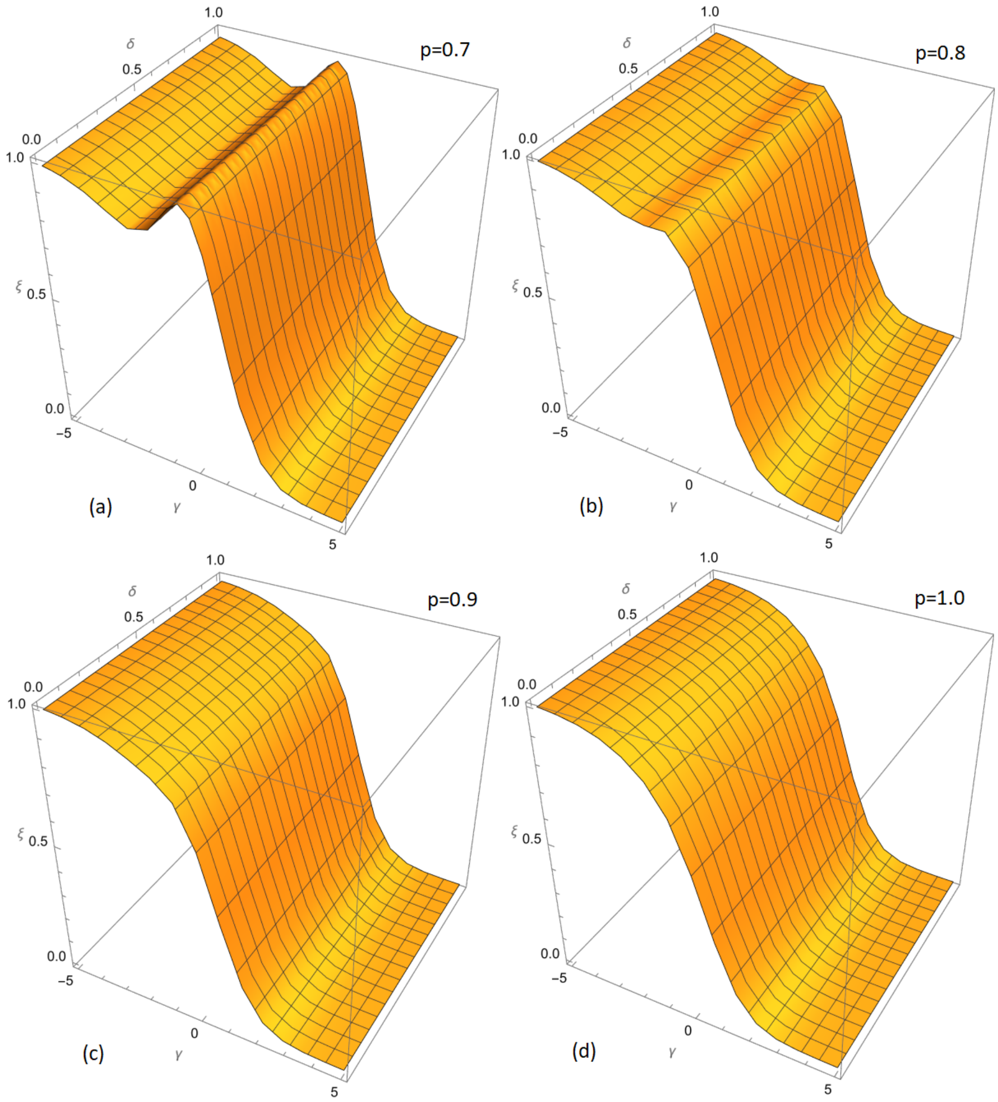

Figure 1. In (**a**), fractional order 0.7, (**b**) fractional order 0.8, (**c**) fractional order 0.9, and (**d**) fractional order 1.0, of the LRPSM of Section 4.1 for $\delta = 0.01$.

In Figure 2, the graphical analysis shifts to the New Iteration Method (NIM) as it tackles Fisher's equation with diverse fractional orders. Subplots (a)–(d) illustrate the NIM results for fractional orders 0.7, 0.8, 0.9, and 1.0, respectively, while maintaining δ at 0.01. These graphical depictions visually showcase the dynamic response of the NIM across different fractional orders.

Table 1. The comparison of different fractional orders of the LRPSM of Section 4.1 for $\delta = 0.01$.

γ	$\mathbf{LRPSM}_{p=0.7}$	$\mathbf{LRPSM}_{p=0.8}$	$\mathbf{LRPSM}_{p=1.0}$	**Exact**	$\mathbf{Error}_{p=0.7}$	$\mathbf{Error}_{p=0.8}$	$\mathbf{Error}_{p=1.0}$
0.1	0.252187	0.250848	0.250125	0.250125	0.00206162	0.000722656	2.604860×10^{-12}
0.1	0.227718	0.226448	0.225763	0.225763	0.00195463	0.000684961	2.061767×10^{-12}
0.2	0.2046	0.203405	0.202761	0.202761	0.00183938	0.000644395	1.489697×10^{-12}
0.3	0.182921	0.181805	0.181203	0.181203	0.00171812	0.000601747	9.117984×10^{-13}
0.4	0.162741	0.161706	0.161148	0.161148	0.00159312	0.000557816	3.50497×10^{-13}
0.5	0.144092	0.143139	0.142626	0.142626	0.0014666	0.000513378	1.743605×10^{-13}
0.6	0.126981	0.12611	0.125641	0.125641	0.00134063	0.00046916	6.464828×10^{-13}
0.7	0.11139	0.110599	0.110173	0.110173	0.00121708	0.000425817	1.054017×10^{-12}
0.8	0.0972797	0.0965661	0.0961822	0.0961822	0.00109758	0.000383914	1.389555×10^{-12}
0.9	0.0845931	0.0839535	0.0836096	0.0836096	0.000983471	0.00034392	1.650179×10^{-12}
1.0	0.0732582	0.0726886	0.0723824	0.0723824	0.000875795	0.000306197	1.836891×10^{-12}

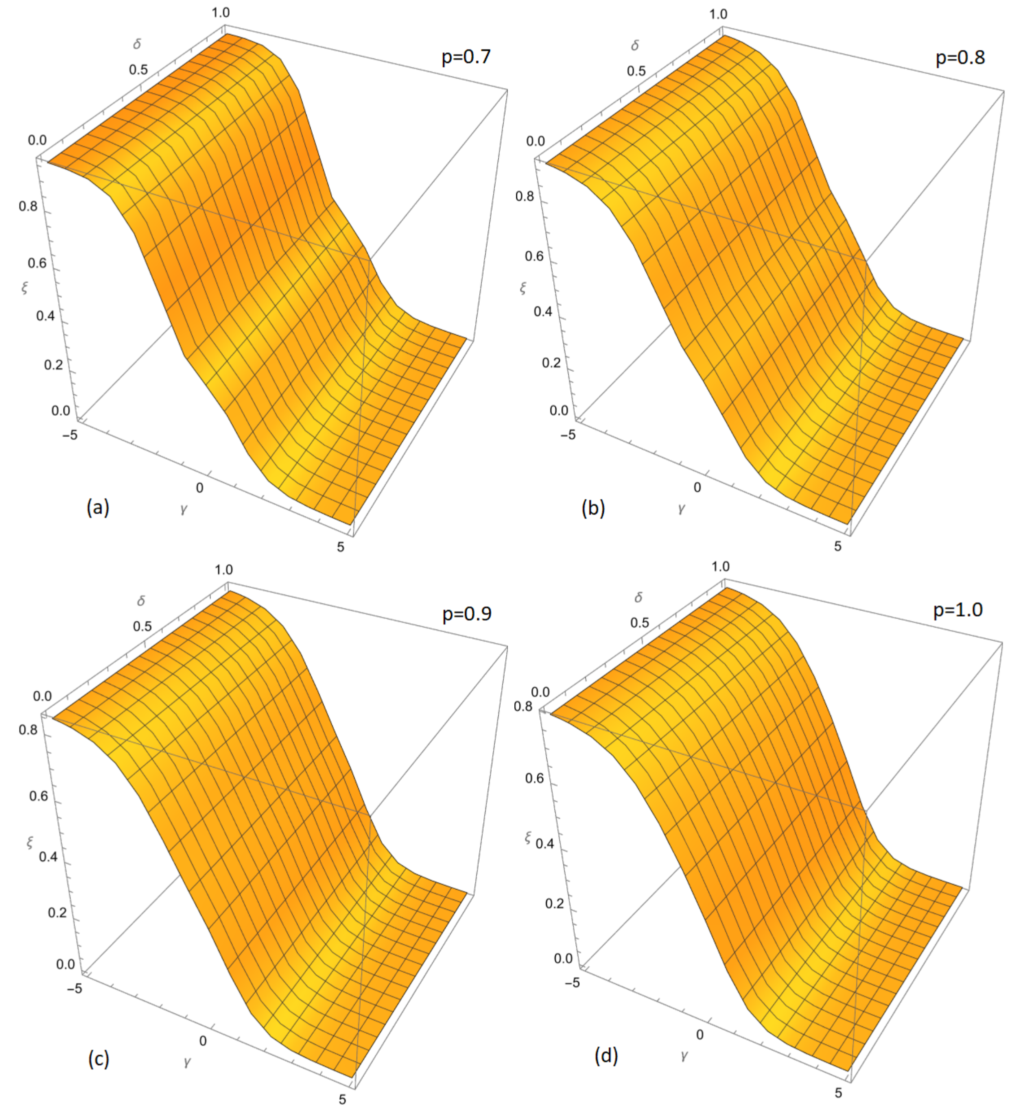

Figure 2. In (**a**), fractional order 0.7, (**b**) fractional order 0.8, (**c**) fractional order 0.9, and (**d**) fractional order 1.0, of the NIM of Section 4.1 for $\delta = 0.01$.

Complementing the graphical analysis, Table 2 compares the NIM solutions for various fractional orders in Section 4.1, with δ fixed at 0.01. This table serves as a quantitative reference for understanding how different fractional orders impact the accuracy and performance of the NIM in the context of solving Fisher's equation. Table 3 gives a comparison of the absolute error of the NIM and LPRSM of Section 4.1 for $\delta = 0.2$. Together, the graphical representations and tables provide a comprehensive exploration of the LRPSM and NIM methodologies in solving Fisher's equation with varying fractional orders, shedding light on these numerical approaches' behavior, accuracy, and efficiency under different conditions.

Table 2. The comparison of different fractional orders of the NIM of Section 4.1 for $\delta = 0.01$.

γ	$\mathbf{NIM}_{p=0.7}$	$\mathbf{NIM}_{p=0.8}$	$\mathbf{NIM}_{p=1.0}$	**Exact**	$\mathbf{Error}_{p=0.7}$	$\mathbf{Error}_{p=0.8}$	$\mathbf{Error}_{p=1.0}$
0.1	0.226411	0.225942	0.225689	0.225763	0.000647684	0.00017922	0.0000745224
0.2	0.203406	0.202943	0.202693	0.202761	0.000645254	0.000182489	0.0000680503
0.3	0.181835	0.181385	0.181141	0.181203	0.000631777	0.000181693	0.000061873
0.4	0.161757	0.161326	0.161092	0.161148	0.000609188	0.000177503	0.0000560092
0.5	0.143205	0.142796	0.142575	0.142626	0.000579417	0.000170587	0.0000504743
0.6	0.126185	0.125802	0.125595	0.125641	0.000544316	0.000161589	0.0000452805
0.7	0.110679	0.110324	0.110133	0.110173	0.000505602	0.000151106	0.000040436
0.8	0.096647	0.0963218	0.0961462	0.0961822	0.000464807	0.000139674	0.0000359452
0.9	0.0840329	0.0837374	0.0835778	0.0836096	0.000423257	0.000127756	0.0000318081
1.0	0.0727644	0.0724981	0.0723544	0.0723824	0.000382057	0.000115742	0.0000280209

Table 3. Comparison of the absolute error of the NIM and LPRSM of Section 4.1 for $\delta = 0.01$.

γ	**Absolute** $\mathbf{Error}_{p=0.7}$	**Absolute** $\mathbf{Error}_{p=0.8}$	**Absolute** $\mathbf{Error}_{p=0.9}$	**Absolute** $\mathbf{Error}_{p=1.0}$
0.1	0.00130694	0.000505741	0.000194723	0.0000745224
0.2	0.00119413	0.000461905	0.000177821	0.0000680503
0.3	0.00108634	0.000420053	0.000161687	0.000061873
0.4	0.000983933	0.000380313	0.00014637	0.0000560092
0.5	0.000887181	0.000342791	0.000131912	0.0000504743
0.6	0.000796309	0.000307571	0.000118344	0.0000452805
0.7	0.000711478	0.00027471	0.000105687	0.000040436
0.8	0.000632774	0.00024424	0.0000939533	0.0000359452
0.9	0.000560213	0.000216164	0.0000831433	0.0000318081
1.0	0.000493738	0.000190455	0.0000732467	0.0000280209

4.2. Problem

Consider the time-Fractional Foam Drainage Equation, given as

$$D_{\delta}^{p}\xi(\gamma,\delta) - \frac{\xi(\gamma,\delta)\partial^2\xi(\gamma,\delta)}{2\partial\gamma^2} + 2\xi^2(\gamma,\delta)\frac{\partial\xi(\gamma,\delta)}{\partial\gamma} - (\frac{\partial\xi(\gamma,\delta)}{\partial\gamma})^2 = 0 \text{ where } \quad 0 < p \leq 1, \tag{27}$$

subject to the following ICs:

$$\xi(\gamma,0) = \sin(x). \tag{28}$$

Implementation of the Laplace Residual Power Series Method

Applying the LT to Equation (27) and making use of Equation (28), we get

$$\xi(\gamma,s)-\frac{\sin(\gamma)}{s}-\frac{1}{2s^{p}}\mathcal{L}_{\delta}[(\mathcal{L}_{\delta}^{-1}\xi(\gamma,s))\times(\mathcal{L}_{\delta}^{-1}\frac{\partial^{2}\xi(\gamma,s)}{2\partial\gamma^{2}})]+\frac{2}{s^{p}}\mathcal{L}_{\delta}[(\mathcal{L}_{\delta}^{-1}\xi^{2}(\gamma,s))\times(\mathcal{L}_{\delta}^{-1}\frac{\partial\xi(\gamma,s)}{\partial\gamma})]$$
$$-\mathcal{L}_{\delta}[(\mathcal{L}_{\delta}^{-1}\frac{\partial\xi\gamma,s}{\partial\gamma})^{2}]=0, \tag{29}$$

and so, the kth truncated term series are

$$\xi(\gamma,s)=\frac{\sin(\gamma)}{s}+\sum_{r=1}^{k}\frac{f_{r}(\gamma,s)}{s^{rp+1}},\quad r=1,2,3,4\cdots. \tag{30}$$

The Laplace residual functions (LRFs) [51] are

$$\mathcal{L}_{\delta}Res(\gamma,s)=\xi(\gamma,s)-\frac{\sin(\gamma)}{s}-\frac{1}{2s^{p}}\mathcal{L}_{\delta}\left[(\mathcal{L}_{\delta}^{-1}\xi(\gamma,s))\times\left(\mathcal{L}_{\delta}^{-1}\frac{\partial^{2}\xi(\gamma,s)}{2\partial\gamma^{2}}\right)\right]$$
$$+\frac{2}{s^{p}}\mathcal{L}_{\delta}\left[(\mathcal{L}_{\delta}^{-1}\xi^{2}(\gamma,s))\times(\mathcal{L}_{\delta}^{-1}\frac{\partial\xi(\gamma,s)}{\partial\gamma})\right]-\mathcal{L}_{\delta}\left[\left(\mathcal{L}_{\delta}^{-1}\frac{\partial\xi\gamma,s}{\partial\gamma}\right)^{2}\right]=0 \tag{31}$$

and the kth LRFs are:

$$\mathcal{L}_{\delta}Res_{k}(\gamma,s)=\xi_{k}(\gamma,s)-\frac{\sin(\gamma)}{s}-\frac{1}{2s^{p}}\mathcal{L}_{\delta}\left[(\mathcal{L}_{\delta}^{-1}\xi_{k}(\gamma,s))\times\left(\mathcal{L}_{\delta}^{-1}\frac{\partial^{2}\xi_{k}(\gamma,s)}{2\partial\gamma^{2}}\right)\right]$$
$$+\frac{2}{s^{p}}\mathcal{L}_{\delta}\left[(\mathcal{L}_{\delta}^{-1}\xi_{k}^{2}(\gamma,s))\times\left(\mathcal{L}_{\delta}^{-1}\frac{\partial\xi_{k}(\gamma,s)}{\partial\gamma}\right)\right]-\mathcal{L}_{\delta}\left[\left(\mathcal{L}_{\delta}^{-1}\frac{\partial\xi_{k}(\gamma,s)}{\partial\gamma}\right)^{2}\right]=0 \tag{32}$$

Now, to determine $f_r(\gamma,s)$, $r=1,2,3,\cdots$, we substitute the rth truncated series Equation (30) into the rth Laplace residual function Equation (32), multiply the resulting equation by s^{rp+1}, and then, recursively solve the relation $\lim_{s\to\infty}(s^{rp+1}\mathcal{L}_{\delta}Res_{\xi,r}(\gamma,s))=0$, $r=1,2,3,\cdots$. The following are the first few terms:

$$f_{1}(\gamma,s)=\frac{1}{4}(1-2\cos(\gamma)+3\cos(2\gamma)+2\cos(3\gamma)), \tag{33}$$

$$f_{2}(\gamma,s)=\frac{1}{16}(-19\sin(\gamma)+24\sin(2\gamma)-3\sin(3\gamma)-68\sin(4\gamma)-20\sin(5\gamma)). \tag{34}$$

and so on.

Putting the values of $f_r(\gamma,s)$, $r=1,2,3,\cdots$, into Equation (30), we get

$$\xi(\gamma,s)=\frac{\sin(\gamma)}{s}+\frac{1}{4s^{p+1}}(1-2\cos(\gamma)+3\cos(2\gamma)+2\cos(3\gamma))$$
$$+\frac{1}{16s^{2p+1}}(-19\sin(\gamma)+24\sin(2\gamma)-3\sin(3\gamma)-68\sin(4\gamma)-20\sin(5\gamma))+\cdots. \tag{35}$$

Using the inverse Laplace transform, we get

$$\xi(\gamma,\delta)=\sin(\gamma)+\frac{\delta^{p}}{\Gamma(p+1)}\left(\frac{1}{4}(1-2\cos(\gamma)+3\cos(2\gamma)+2\cos(3\gamma))\right)$$
$$+\frac{\delta^{2p}}{\Gamma(2p+1)}\left(\frac{1}{16}(-19\sin(\gamma)+24\sin(2\gamma)-3\sin(3\gamma)-68\sin(4\gamma)-20\sin(5\gamma))\right)+\cdots. \tag{36}$$

Implementation of New Iteration Method

Applying the RL integral to Equation (27), we get the equivalent form:

$$\xi(\gamma,\delta) = \sin(\gamma) - \Re_{\delta}^{p}\left[\frac{\xi(\gamma,\delta)\partial^2\xi(\gamma,\delta)}{2\partial\gamma^2} - 2\xi^2(\gamma,\delta)\frac{\partial\xi(\gamma,\delta)}{\partial\gamma} + \left(\frac{\partial\xi(\gamma,\delta)}{\partial\gamma}\right)^2\right] \tag{37}$$

According to the NIM procedure, we get the following few terms:

$$\begin{aligned}
&\xi_0(\gamma,\delta) = \sin(\gamma),\\
&\xi_1(\gamma,\delta) = \frac{\delta^p(1-2\cos(\gamma)+3\cos(2\gamma)+2\cos(3\gamma))}{4\Gamma[1+p]},\\
&\xi_2(\gamma,\delta) = \frac{\delta(2p)}{16\Gamma[1+p]^4)}\Big(-\delta^p(-19+2\cos(\gamma)+7\cos(2\gamma))\\
&-27\cos(4\gamma)+48\cos(5\gamma)+63\cos(6\gamma)+14\cos(7\gamma))\Gamma[1+p]+\delta^{2p}(1-2\cos(\gamma)\\
&+3\cos(2\gamma)+2\cos(3\gamma))^2(-\sin(\gamma)+3(\sin(2\gamma)+\sin(3\gamma)))\\
&-\Gamma[1+p]^2(19\sin(\gamma)-24\sin(2\gamma)+3\sin(3\gamma)\\
&+68\sin(4\gamma)+20\sin(5\gamma))\Big)
\end{aligned} \tag{38}$$

By the NIM algorithm, the final solution is

$$\xi(\gamma,\delta) = \xi_0(\gamma,\delta) + \xi_1(\gamma,\delta) + \xi_2(\gamma,\delta) + \cdots \tag{39}$$

$$\begin{aligned}
\xi(\gamma,\delta) =& \sin(\gamma) + \frac{\delta^p(1-2\cos(\gamma)+3\cos(2\gamma)+2\cos(3\gamma))}{4\Gamma[1+p]}\\
&+\frac{\delta^{2p}}{16\Gamma[1+p]^4)}\Big(-\delta^p(-19+2\cos(\gamma)+7\cos(2\gamma))\\
&-27\cos(4\gamma)+48\cos(5\gamma)+63\cos(6\gamma)+14\cos(7\gamma))\Gamma[1+p]+\delta^{2p}(1-2\cos(\gamma)\\
&+3\cos(2\gamma)+2\cos(3\gamma))^2(-\sin(\gamma)+3(\sin(2\gamma)+\sin(3\gamma)))\\
&-\Gamma[1+p]^2(19\sin(\gamma)-24\sin(2\gamma)+3\sin(3\gamma)\\
&+68\sin(4\gamma)+20\sin(5\gamma))\Big)+\cdots.
\end{aligned} \tag{40}$$

In Figure 3, the graphical representation illustrates the Laplace Residual Power Series Method (LRPSM) behavior for varying fractional orders. Panel (a) showcases the results for a fractional order of 0.7, while Panel (b) depicts the case for a fractional order of 0.8. Moving on to Panel (c), the behavior of the LRPSM is shown for a fractional order of 0.9. Finally, in Panel (d), the behavior of the LRPSM for a fractional order of 1.0 is presented. These plots offer insights into the impact of different fractional orders on the solutions obtained using the LRPSM for the Foam Drainage Equation with a given parameter $\delta = 0.01$, as outlined in Section 4.2.

Table 4 presents a quantitative comparison of different fractional orders within the LRPSM for the same problem. Specifically, it compiles the results obtained using the LRPSM for various fractional orders, considering a fixed value of $\delta = 0.01$. This table offers a comprehensive overview of how the choice of the fractional order influences the solutions obtained via the LRPSM for the Foam Drainage Equation.

Figure 4 further extends the analysis, this time focusing on the New Iteration Method (NIM) applied to the same Foam Drainage Equation with $\delta = 0.01$. Panel (a) provides insights into the behavior of the NIM for a fractional order of 0.7, followed by Panel (b) for a fractional order of 0.8. Panel (c) illustrates the results for a fractional order of 0.9, while Panel (d) completes the overview with the case of a fractional order of 1.0.

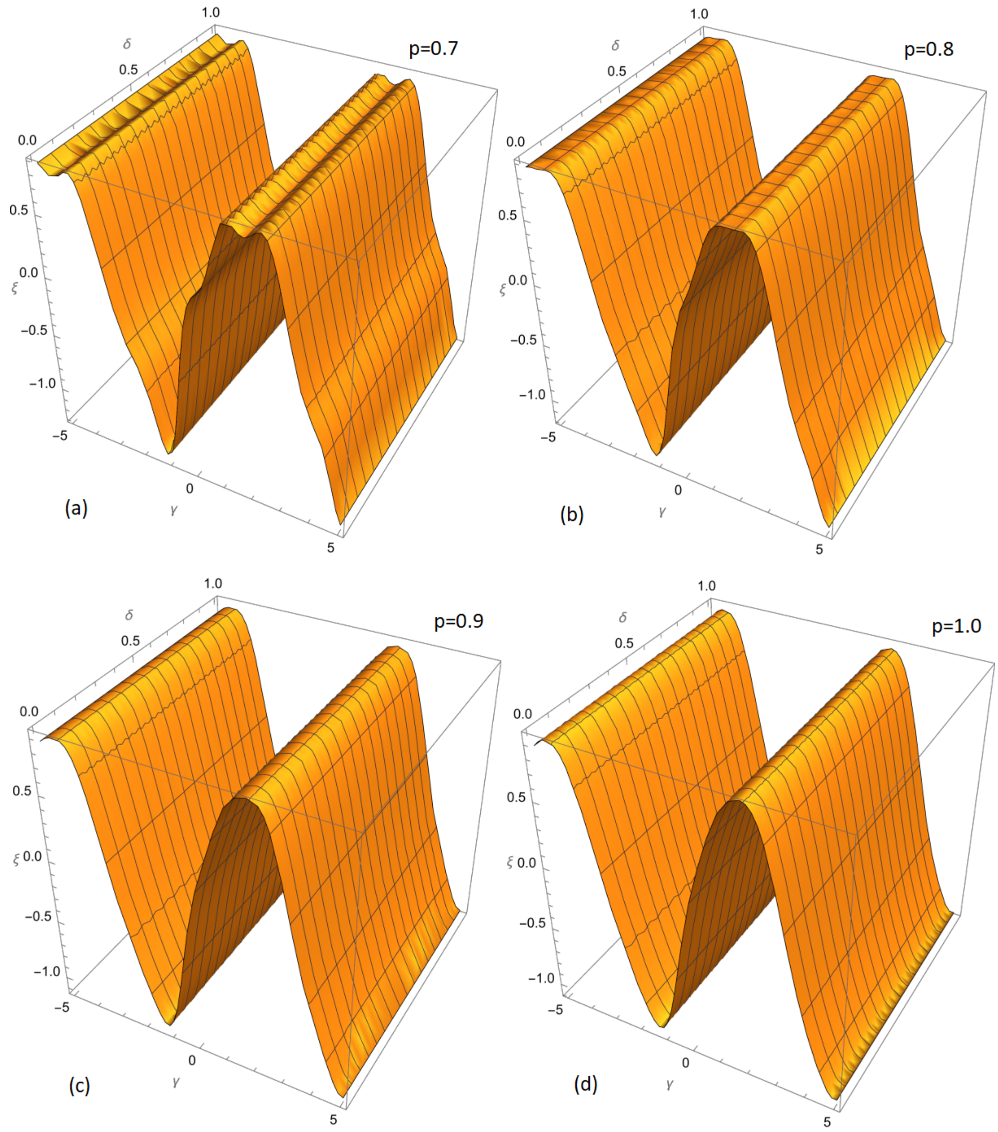

Figure 3. In (**a**), fractional order 0.7, (**b**) fractional order 0.8, (**c**) fractional order 0.9, and (**d**) fractional order 1.0, of the LRPSM of Section 4.2 for $\delta = 0.2$.

Table 4. The comparison of different fractional orders of the LRPSM of Section 4.2 for $\delta = 0.2$.

γ	LRPSM Solution$_{p=0.7}$	LRPSM Solution$_{p=0.8}$	LRPSM Solution$_{p=0.9}$	LRPSM Solution$_{p=1.0}$
0.1	0.139405	0.124925	0.11542	0.109379
0.2	0.231577	0.220253	0.21232	0.207111
0.3	0.320084	0.312312	0.306363	0.302299
0.4	0.404716	0.400536	0.396804	0.394103
0.5	0.485218	0.484404	0.48296	0.481738
0.6	0.561253	0.563417	0.564193	0.564472
0.7	0.632388	0.637085	0.639911	0.641622
0.8	0.698122	0.704926	0.709556	0.712552
0.9	0.757925	0.766468	0.7726	0.776672
1.0	0.811291	0.821258	0.828551	0.833436

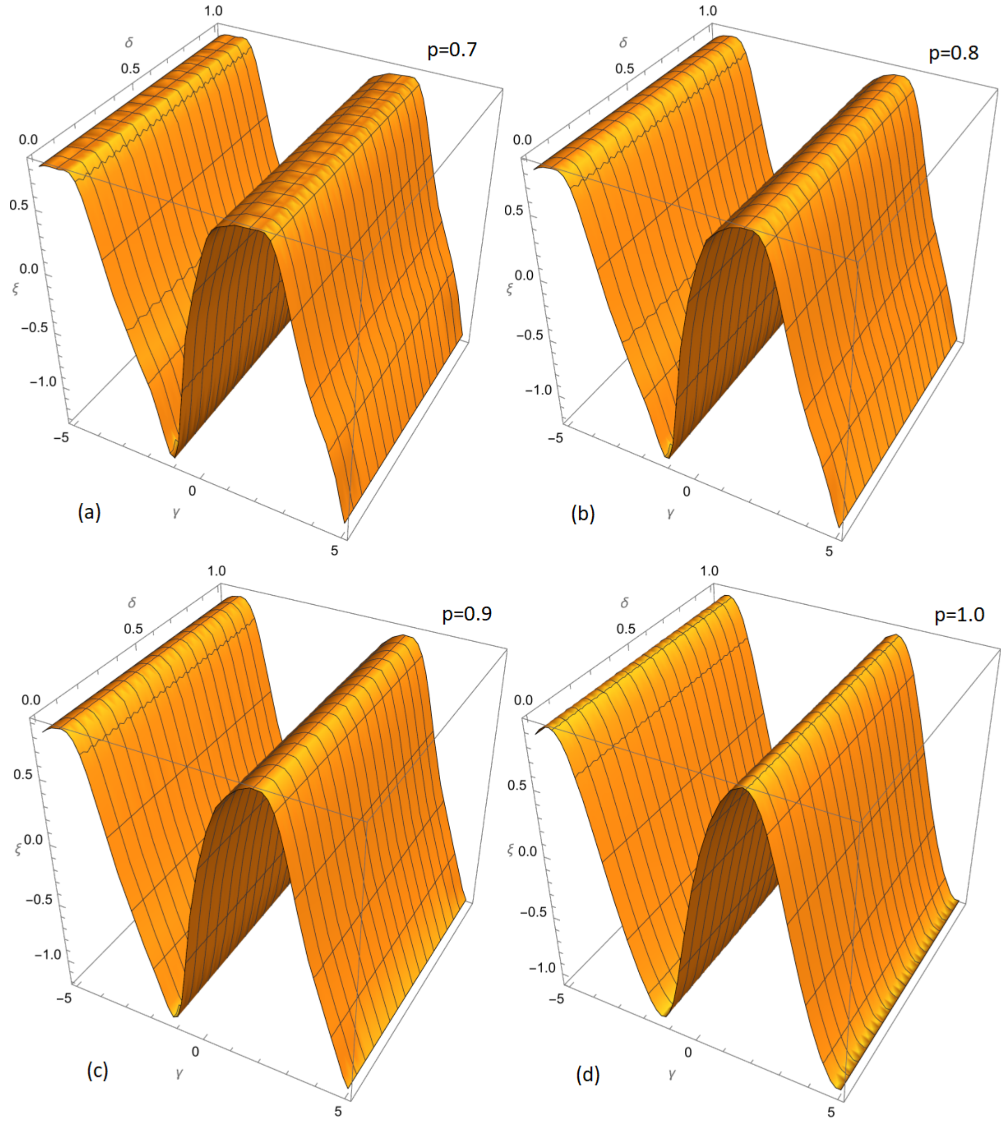

Figure 4. In (**a**), fractional order 0.7, (**b**) fractional order 0.8, (**c**) fractional order 0.9, and (**d**) fractional order 1.0, of the NIM of Section 4.2 for $\delta = 0.2$.

Table 5 complements the graphical analyses by offering a tabular comparison of different fractional orders within the NIM for the same example. This table summarizes the numerical results obtained using the NIM for various fractional orders, considering the fixed value of $\delta = 0.01$. Collectively, these visual and tabular representations provide a comprehensive exploration of the influence of fractional orders on the solutions obtained through the LRPSM and NIM for the Foam Drainage Equation in Section 4.2. Table 6 gives a comparison of the absolute error of the NIM and LPRSM of Section 4.2 for $\delta = 0.2$

Table 5. The comparison of different fractional orders of the NIM of Section 4.2 for $\delta = 0.2$.

γ	NIM Solution$_{p=0.7}$	NIM Solution$_{p=0.8}$	NIM Solution$_{p=0.9}$	NIM Solution$_{p=1.0}$
0.1	0.141605	0.125701	0.115687	0.109469
0.2	0.235882	0.221741	0.212825	0.207279
0.3	0.325946	0.314318	0.30704	0.302524
0.4	0.411365	0.402798	0.397565	0.394355
0.5	0.491795	0.486633	0.483707	0.481986
0.6	0.566952	0.565347	0.564841	0.564687
0.7	0.636596	0.638515	0.640392	0.641782
0.8	0.700512	0.705748	0.709834	0.712645
0.9	0.758494	0.76668	0.772675	0.776698
1.0	0.810334	0.820954	0.828453	0.833404

Table 6. Comparison of the absolute error of the NIM and LPRSM of Section 4.2 for $\delta = 0.2$.

γ	Absolute Error$_{p=0.7}$	Absolute Error$_{p=0.8}$	Absolute Error$_{p=0.9}$	Absolute Error$_{p=1.0}$
0.1	0.0000909551	0.000019951	4.283578×10^{-6}	9.0292663×10^{-7}
0.2	0.000171151	0.000037349	7.999739×10^{-6}	1.684364×10^{-6}
0.3	0.000228606	0.0000497577	0.0000106445	2.239945×10^{-6}
0.4	0.000256211	0.0000556725	0.0000119004	2.503296×10^{-6}
0.5	0.000251675	0.0000546336	0.0000116729	2.454922×10^{-6}
0.6	0.000217807	0.0000472723	0.0000100992	2.123858×10^{-6}
0.7	0.000161866	0.0000351633	7.515498×10^{-6}	1.580830×10^{-6}
0.8	0.0000941308	0.0000205158	4.3916752×10^{-6}	9.244249×10^{-7}
0.9	0.0000259664	5.765185×10^{-6}	1.244783×10^{-6}	2.6306740×10^{-7}
1.0	0.0000321962	6.853422×10^{-6}	1.450543×10^{-6}	3.037118×10^{-7}

4.3. Problem

Consider the time-fractional Fisher's equation given as:

$$D_{\delta}^{p}\xi(\gamma,\delta) - \frac{\partial^2 \xi(\gamma,\delta)}{\partial \gamma^2} - \xi(\gamma,\delta) + \xi^2(\gamma,\delta) = 0, \quad \text{where} \quad 0 < p \leq 1, \tag{41}$$

subject to the following ICs:

$$\xi(\gamma,0) = \lambda. \tag{42}$$

The exact solution is

$$\xi(\gamma,\delta) = \frac{\lambda e^{\gamma}}{-\lambda + \lambda e^{\delta} + 1}.$$

Implementation of the Laplace Residual Power Series Method

Applying the LT to Equation (41) and making use of Equation (42), we get

$$\xi(\gamma,s) - \frac{\lambda}{s} - \frac{1}{s^p}\frac{\partial^2 \xi(\gamma,s)}{\partial \gamma^2} - \frac{1}{s^p}\xi(\gamma,s) + \frac{1}{s^p}\mathcal{L}_{\delta}[(\mathcal{L}_{\delta}^{-1}[\xi(\gamma,s)])^2] = 0, \tag{43}$$

and so, the kth truncated term series are

$$\xi(\gamma,s)=\frac{\lambda}{s}+\sum_{r=1}^{k}\frac{f_r(\gamma,s)}{s^{rp+1}},\ \ r=1,2,3,4\cdots. \tag{44}$$

The Laplace residual functions (LRFs) [54] are

$$\mathcal{L}_\delta Res(\gamma,s)=\xi(\gamma,s)-\frac{\lambda}{s}-\frac{1}{s^p}\frac{\partial^2\xi(\gamma,s)}{\partial\gamma^2}-\frac{1}{s^p}\xi(\gamma,s)+\frac{1}{s^p}\mathcal{L}_\delta[(\mathcal{L}_\delta^{-1}[\xi(\gamma,s)])^2]=0, \tag{45}$$

and the kth LRFs are:

$$\mathcal{L}_\delta Res_k(\gamma,s)=\xi_k(\gamma,s)-\frac{\lambda}{s}-\frac{1}{s^p}\frac{\partial^2\xi_k(\gamma,s)}{\partial\gamma^2}-\frac{1}{s^p}\xi_k(\gamma,s)+\frac{1}{s^p}\mathcal{L}_\delta[(\mathcal{L}_\delta^{-1}[\xi_k(\gamma,s)])^2]=0. \tag{46}$$

Now, to determine $f_r(\gamma,s)$, $r=1,2,3,\cdots$, we substitute the rth truncated series Equation (44) into the rth Laplace residual function Equation (46), multiply the resulting equation by s^{rp+1}, and then, recursively solve the relation $\lim_{s\to\infty}(s^{rp+1}\mathcal{L}_\delta Res_{\xi,r}(\gamma,s))=0$, $r=1,2,3,\cdots$. The following are the first few terms:

$$f_1(\gamma,s)=\lambda-\lambda^2, \tag{47}$$

$$f_2(\gamma,s)=2\lambda^3-3\lambda^2+\lambda, \tag{48}$$

and so on.

Putting the values of $f_r(\gamma,s)$, $r=1,2,3,\cdots$, into Equation (44), we get

$$\xi(\gamma,s)=\frac{\lambda}{s}+\frac{1}{s^{p+1}}\left(\lambda-\lambda^2\right)+\frac{1}{s^{2p+1}}\left(2\lambda^3-3\lambda^2+\lambda\right)+\cdots. \tag{49}$$

Using the inverse Laplace transform, we get

$$\xi(\gamma,\delta)=\lambda+\frac{\delta^p}{\Gamma(p+1)}\left(\lambda-\lambda^2\right)+\frac{\delta^{2p}}{\Gamma(2p+1)}\left(2\lambda^3-3\lambda^2+\lambda\right)+\cdots \tag{50}$$

Implementation of New Iteration Method

Applying the RL integral to Equation (41), we get the equivalent form:

$$\xi(\gamma,\delta)=\lambda-\mathfrak{R}_\delta^p[\frac{\partial^2\xi(\gamma,\delta)}{\partial\gamma^2}+\xi(\gamma,\delta)-\xi^2(\gamma,\delta)] \tag{51}$$

According to the NIM procedure, we obtain as

$$\begin{aligned}
&\xi_0(\gamma,\delta)=\lambda,\\
&\xi_1(\gamma,\delta)=-\frac{(\lambda-1)\lambda\delta^p}{\Gamma(p+1)},\\
&\xi_2(\gamma,\delta)=(\lambda-1)\lambda\delta^{2p}\left(\frac{2\lambda-1}{\Gamma(2p+1)}-\frac{(\lambda-1)\lambda4^p\delta^p\Gamma\left(p+\frac{1}{2}\right)}{\sqrt{\pi}\Gamma(p+1)\Gamma(3p+1)}\right)
\end{aligned} \tag{52}$$

By the NIM algorithm, the final solution is

$$\xi(\gamma,\delta)=\xi_0(\gamma,\delta)+\xi_1(\gamma,\delta)+\xi_2(\gamma,\delta)+\cdots \tag{53}$$

$$\xi(\gamma,\delta) = \lambda - \frac{(\lambda-1)\lambda\delta^p}{\Gamma(p+1)} + (\lambda-1)\lambda\delta^{2p}\left(\frac{2\lambda-1}{\Gamma(2p+1)} - \frac{(\lambda-1)\lambda 4^p\delta^p\Gamma\left(p+\frac{1}{2}\right)}{\sqrt{\pi}\Gamma(p+1)\Gamma(3p+1)}\right) + \cdots \quad (54)$$

The tables and figures presented provide a comprehensive comparative analysis of the LRPSM and the NIM for addressing Section 4.3 with varying fractional orders and specific parameter settings. Table 7 compares different fractional orders for the LRPSM when $\delta = 0.1$ and $\gamma = 0.01$. It systematically assesses how various fractional orders impact the LRPSM solutions for Section 4.3. This table is a valuable resource for understanding the influence of fractional order selection on solution accuracy. Figure 5 further visualizes the LRPSM solutions for Section 4.3 under varying fractional orders, ranging from 0.7 to 1.0, all within the context of $\delta = 0.1$ and $\gamma = 0.01$. The subfigures (a)–(d) provide a clear representation of how the choice of fractional order affects the convergence and behavior of the LRPSM solutions.

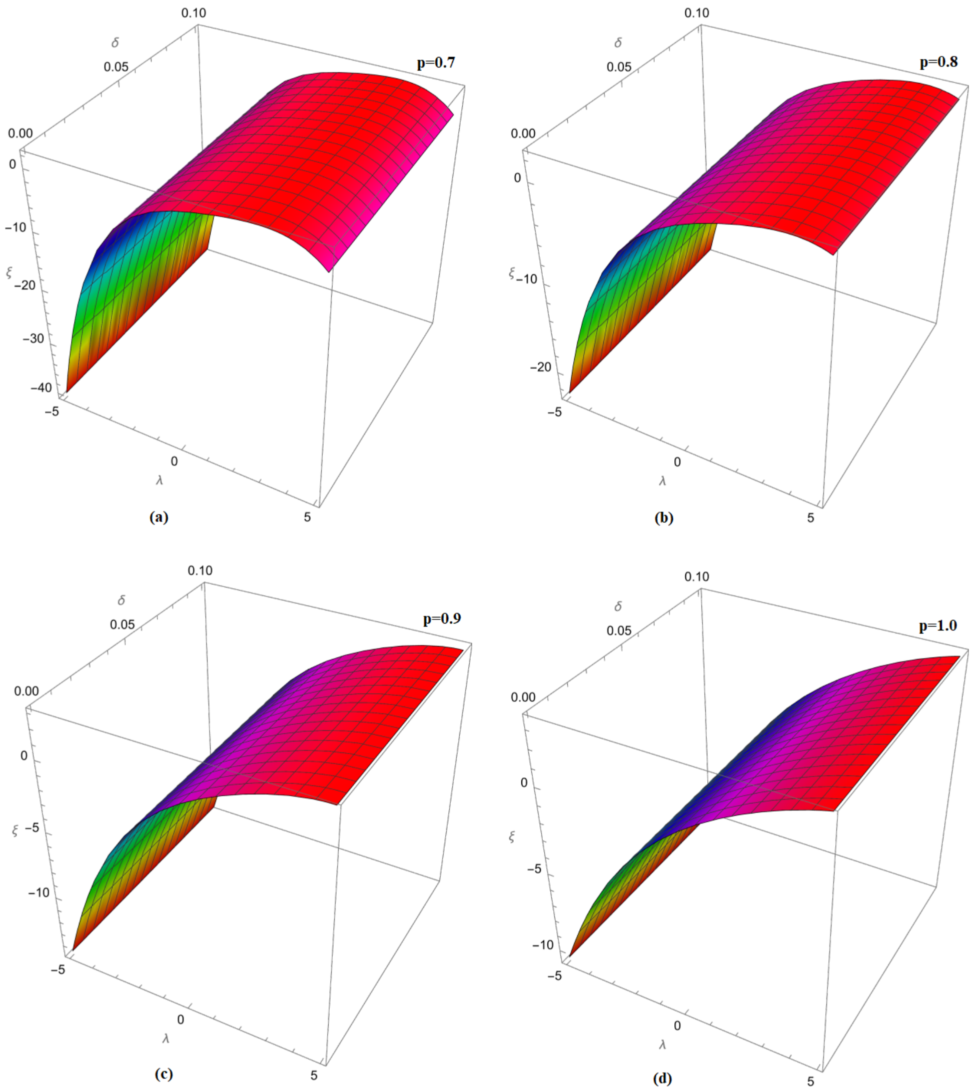

Figure 5. In (**a**), fractional order 0.7, (**b**) fractional order 0.8, (**c**) fractional order 0.9, and (**d**) fractional order 1.0, of the LRPSM of Section 4.3 for $\delta = 0.1$ and $\gamma = 0.01$.

Table 7. The comparison of different fractional orders of the LRPSM of Section 4.3 for $\delta = 0.1$ and $\gamma = 0.01$.

λ	$\mathbf{LRPSM}_{p=0.7}$	$\mathbf{LRPSM}_{p=0.8}$	$\mathbf{LRPSM}_{p=1.0}$	**Exact**	$\mathbf{Error}_{p=0.7}$	$\mathbf{Error}_{p=0.8}$	$\mathbf{Error}_{p=1.0}$
0.1	0.104036	0.102459	0.100904	0.100904	0.00313278	0.00155565	2.454758×10^{-12}
0.2	0.207133	0.204358	0.201605	0.201605	0.00552841	0.00275275	3.689698×10^{-11}
0.3	0.309307	0.3057	0.302104	0.302104	0.0072029	0.00359625	5.320094×10^{-11}
0.4	0.410574	0.406493	0.402402	0.402402	0.00817191	0.00409101	3.745714×10^{-11}
0.5	0.510951	0.506742	0.5025	0.5025	0.00845072	0.00424182	2.082778×10^{-13}
0.6	0.610452	0.606451	0.602398	0.602398	0.00805422	0.00405344	3.774192×10^{-11}
0.7	0.709093	0.705626	0.702096	0.702096	0.00699694	0.0035305	5.319811×10^{-11}
0.8	0.806888	0.804273	0.801595	0.801595	0.00529303	0.00267762	3.670286×10^{-11}
0.9	0.903853	0.902396	0.900896	0.900896	0.00295625	0.0014993	2.345568×10^{-12}

Table 8 also makes a comparison, but focuses on the New Iteration Method (NIM). It compares different fractional orders when $\delta = 0.1$ and $\gamma = 0.01$, providing a detailed insight into how fractional orders impact the NIM solutions for Section 4.3. Figure 6 complements the analysis by visually representing the NIM solutions for Section 4.3 across fractional orders ranging from 0.7 to 1.0, all within the given parameter settings of $\delta = 0.1$ and $\gamma = 0.01$. The subfigures (a)–(d) help in grasping the visual nuances of the NIM solutions.

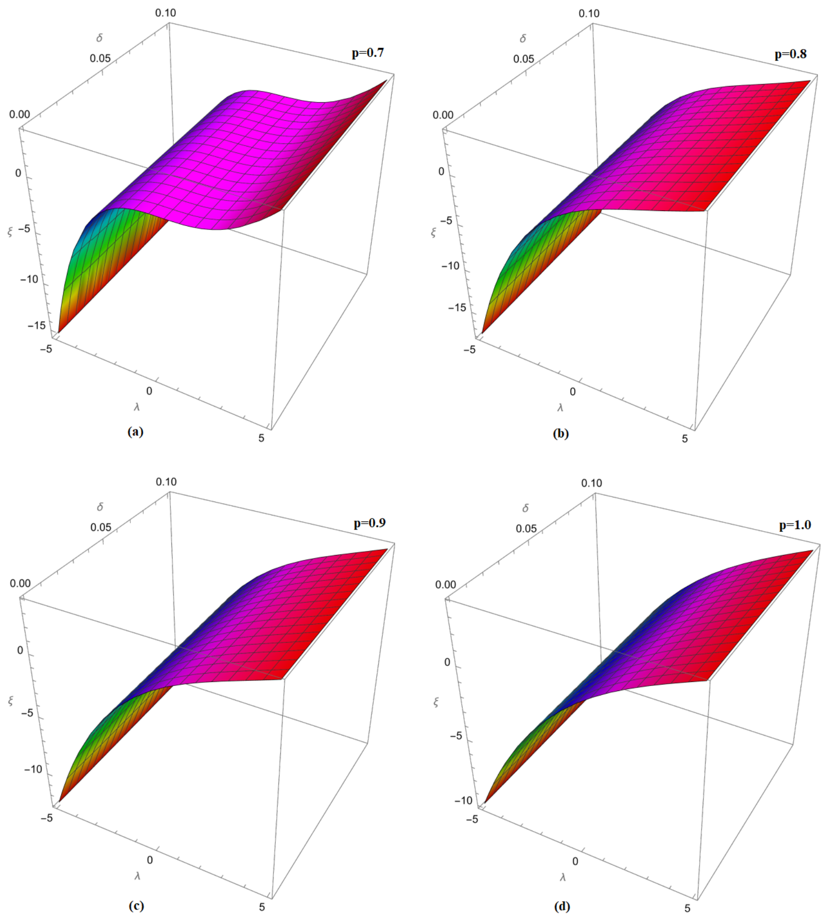

Figure 6. In (**a**), fractional order 0.7, (**b**) fractional order 0.8, (**c**) fractional order 0.9, and (**d**) fractional order 1.0, of the NIM of Section 4.3 for $\delta = 0.1$ and $\gamma = 0.01$.

Table 8. The comparison of different fractional orders of the NIM of Section 4.3 for $\delta = 0.1$ and $\gamma = 0.01$.

λ	$\mathbf{NIM}_{p=0.7}$	$\mathbf{NIM}_{p=0.8}$	$\mathbf{NIM}_{p=1.0}$	**Exact**	$\mathbf{Error}_{p=0.7}$	$\mathbf{Error}_{p=0.8}$	$\mathbf{Error}_{p=1.0}$
0.1	0.104035	0.102459	0.100904	0.100904	0.00313113	0.00155535	9.597545×10^{-9}
0.2	0.207132	0.204357	0.201605	0.201605	0.00552675	0.00275245	9.563103×10^{-9}
0.3	0.309306	0.3057	0.302104	0.302104	0.00720193	0.00359607	5.546799×10^{-9}
0.4	0.410574	0.406493	0.402402	0.402402	0.00817163	0.00409095	1.562542×10^{-9}
0.5	0.510951	0.506742	0.5025	0.5025	0.00845072	0.00424182	2.082778×10^{-9}
0.6	0.610452	0.606451	0.602398	0.602398	0.00805395	0.00405339	1.637741×10^{-9}
0.7	0.709092	0.705626	0.702096	0.702096	0.00699598	0.00353032	5.653198×10^{-9}
0.8	0.806887	0.804273	0.801595	0.801595	0.00529138	0.00267731	9.636702×10^{-9}
0.9	0.903851	0.902395	0.900896	0.900896	0.0029546	0.00149899	9.602345×10^{-9}

These tables and figures serve as valuable references for researchers and practitioners seeking to make informed decisions regarding the choice of the method and fractional order for addressing Section 4.3 in the context of the Fisher equation. They contribute to understanding how different parameters and methods influence the accuracy and convergence of the solutions, enhancing the applicability of these mathematical techniques to practical problems.

5. Conclusions

In conclusion, our research showed that the Laplace Residual Power Series Method (LRPSM) and the New Iteration Method (NIM) are equally successful and flexible in resolving challenging partial differential equations containing the Caputo operator. We successfully discovered precise and effective solutions to the Foam Drainage Equation and the nonlinear time-fractional Fisher's equation, providing new insights into the behavior of these complex mathematical models. The correctness of our technique was further shown by using figures and tables to demonstrate it. This study not only advances the field of mathematical analysis, but also highlights how crucial it is to investigate cutting-edge approaches to challenging issues in various scientific fields.

Our results demonstrate the potential of the New Iteration Method and the Laplace Residual Power Series Method as useful methods for solving fractional partial differential equations. Combining these approaches offers a solid way of dealing with fractional derivative equations and nonlinear dynamics, enhancing our analytical capacity to describe real-world occurrences. Our comprehension of complicated systems will advance as we use these strategies, and our capacity to tackle challenging mathematical and physical issues will grow.

In summary, this study emphasized the value of novel strategies for solving mathematical problems and calls for more research into the Laplace Residual Power Series and New Iteration Method for a broader range of issues. The Foam Drainage Equation and the Nonlinear Time-Fractional Fisher's Equation were successfully solved, demonstrating the promise of these techniques and opening the door for further developments in mathematical research and its many applications.

Author Contributions: Conceptualization, A.B.M.A.; methodology, A.B.M.A.; software, A.B.M.A.; validation, G.A.; formal analysis, A.B.M.A.; writing—original draft preparation, A.B.M.A.; writing—review and editing, G.A. All authors have read and agreed to the published version of the manuscript.

Funding: This research received no external funding.

Data Availability Statement: The numerical data used to support the findings of this study are included within the article.

Acknowledgments: The authors would like to extend their sincere appreciation to the Researchers Supporting Project number (RSPD2023R920), King Saud University, Saudi Arabia.

Conflicts of Interest: The authors declare that there is no conflict of interest regarding the publication of this article.

References

1. Oldham, K.; Spanier, J. *The Fractional Calculus Theory and Applications of Differentiation and Integration to Arbitrary Order*; Elsevier: Berlin/Heidelberg, Germany, 1974.
2. Caputo, M. Linear models of dissipation whose Q is almost frequency independent-II. *Geophys. J. Int.* **1967**, *13*, 529–539. [CrossRef]
3. Schneider, W.R.; Wyss, W. Fractional diffusion and wave equations. *J. Math. Phys.* **1989**, *30*, 134–144. [CrossRef]
4. Yasmin, H.; Aljahdaly, N.H.; Saeed, A.M. Investigating Symmetric Soliton Solutions for the Fractional Coupled Konno-Onno System Using Improved Versions of a Novel Analytical Technique. *Mathematics* **2023**, *11*, 2686. [CrossRef]
5. Yasmin, H.; Aljahdaly, N.H.; Saeed, A.M. Investigating Families of Soliton Solutions for the Complex Structured Coupled Fractional Biswas-Arshed Model in Birefringent Fibers Using a Novel Analytical Technique. *Fractal Fract.* **2023**, *7*, 491. [CrossRef]
6. Podlubny, I. *Fractional Differential Equations: An Introduction to Fractional Derivatives, Fractional Differential Equations, to Methods of Their Solution and Some of Their Applications*; Elsevier: Berlin/Heidelberg, Germany, 1998.
7. Jawarneh, Y.; Yasmin, H.; Al-Sawalha, M.M.; Khan, A. Numerical analysis of fractional heat transfer and porous media equations within Caputo-Fabrizio operator. *AIMS Math.* **2023**, *8*, 26543–26560. [CrossRef]
8. Huang, F.; Liu, F. The fundamental solution of the space-time-fractional advection-dispersion equation. *J. Appl. Math. Comput.* **2005**, *18*, 339–350. [CrossRef]
9. Jin, H.; Wang, Z.; Wu, L. Global dynamics of a three-species spatial food chain model. *J. Differ. Equ.* **2022**, *333*, 144–183. [CrossRef]
10. Jawarneh, Y.; Al-Sawalha, M.M.; Khan, A. Fractional comparative analysis of Camassa-Holm and Degasperis-Procesi equations. *AIMS Math.* **2023**, *8*, 25845–25862. [CrossRef]
11. Li, H.; Peng, R.; Wang, Z. On a Diffusive Susceptible-Infected-Susceptible Epidemic Model with Mass Action Mechanism and Birth-Death Effect: Analysis, Simulations, and Comparison with Other Mechanisms. *SIAM J. Appl. Math.* **2018**, *78*, 2129–2153. [CrossRef]
12. Sunthrayuth, P.; Aljahdaly, N.H.; Ali, A.; Shah, R.; Mahariq, I.; Tchalla, A.M. ψ-Haar wavelet operational matrix method for fractional relaxation-oscillation equations containing ψ-Caputo fractional derivative. *J. Funct. Spaces* **2021**, *2021*, 7117064. [CrossRef]
13. Odibat, Z.M.; Momani, S. Application of variational iteration method to nonlinear differential equations of fractional order. *Int. J. Nonlinear Sci. Numer. Simul.* **2006**, *7*, 27–34. [CrossRef]
14. Momani, S.; Odibat, Z. Analytical solution of a time-fractional Navier-Stokes equation by Adomian decomposition method. *Appl. Math. Comput.* **2006**, *177*, 488–494. [CrossRef]
15. Kbiri, A.M.; Nonlaopon, K.; Zidan, A.M.; Khan, A. Analytical investigation of fractional-order Cahn-Hilliard and gardner equations using two novel techniques. *Mathematics* **2022**, *10*, 1643. [CrossRef]
16. Odibat, Z.M.; Momani, S. Approximate solutions for boundary value problems of time-fractional wave equation. *Appl. Math. Comput.* **2006**, *181*, 767–774. [CrossRef]
17. Marinca, V. An approximate solution for one-dimensional weakly nonlinear oscillations. *Int. J. Nonlinear Sci. Numer. Simul.* **2002**, *3*, 107–120. [CrossRef]
18. Hao, T.H. Search for variational principles in electrodynamics by Lagrange method. *Int. J. Nonlinear Sci. Numer. Simul.* **2005**, *6*, 209–210. [CrossRef]
19. Momani, S. An explicit and numerical solutions of the fractional KdV equation. *Math. Comput. Simul.* **2005**, *70*, 110–118. [CrossRef]
20. Momani, S.; Abuasad, S. Application of He's variational iteration method to Helmholtz equation. *Chaos Solitons Fractals* **2006**, *27*, 1119–1123. [CrossRef]
21. Momani, S.; Odibat, Z. Homotopy perturbation method for nonlinear partial differential equations of fractional order. *Phys. Lett. A* **2007**, *365*, 345–350. [CrossRef]
22. Arikoglu, A.; Ozkol, I. Solution of fractional differential equations by using differential transform method. *Chaos Solitons Fractals* **2007**, *34*, 1473–1481. [CrossRef]
23. Odibat, Z.; Momani, S. Modified homotopy perturbation method: Application to quadratic Riccati differential equation of fractional order. *Chaos Solitons Fractals* **2008**, *36*, 167–174. [CrossRef]
24. Wang, B.; Zhang, Y.; Zhang, W. A Composite Adaptive Fault-Tolerant Attitude Control for a Quadrotor UAV with Multiple Uncertainties. *J. Syst. Sci. Complex.* **2022**, *35*, 81–104. [CrossRef]
25. Ali, T.A.A.; Xiao, Z.; Jiang, H.; Li, B. A Class of Digital Integrators Based on Trigonometric Quadrature Rules. *IEEE Trans. Ind. Electron.* **2023**, 1–11. [CrossRef]
26. Guo, C.; Hu, J.; Hao, J.; Celikovsky, S.; Hu, X. Fixed-time safe tracking control of uncertain high-order nonlinear pure-feedback systems via unified transformation functions. *Kybernetika* **2023**, *59*, 342–364. [CrossRef]
27. Weaire, D.L.; Hutzler, S. *The Physics of Foams*; Oxford University Press: Oxford, UK, 2001.

28. Rossen, W.; Prud, H.R.; Khan, S. Foams: Theory, measurements and applications. *Foam. Enhanc. Oil Recovery* **1996**, *57*, 413–464.
29. Bikerman, J. (Ed.) General. Foam films. In *Foams*; Springer: Berlin/Heidelberg, Germany, 1973; pp. 1–32.
30. Stone, H.; Koehler, S.; Hilgenfeldt, S.; Dur, M. Perspectives on foam drainage and the influence of interfacial rheology. *J. Phys. Condens. Matter.* **2002**, *15*, S283. [CrossRef]
31. Hilgenfeldt, S.; Koehler, S.A.; Stone, H.A. Dynamics of coarsening foams: Accelerated and self-limiting drainage. *Phys. Rev. Lett.* **2001**, *86*, 4704. [CrossRef]
32. Schultz, O.; des Ligneris, A.; Haider, O.; Starke, P. Fatigue behavior, strength, and failure of aluminum foam. *Adv. Energy Mater.* **2000**, *2*, 215–218. [CrossRef]
33. Fisher, R.A. The wave of advance of advantageous genes. *Ann. Eugen.* **1937**, *7*, 353–369. [CrossRef]
34. Alquran, M.; Al-Khaled, K.; Sardar, T.; Chattopadhyay, J. Revisited Fishers equation in a new outlook: A fractional derivative approach. *Physica A* **2015**, *438*, 81–93. [CrossRef]
35. Ammerman, A.J.; Cavalli-Sforza, L.L. *The Neolithic Transition and the Genetics of Population in Europe*; Princeton University Press: Princeton, NJ, USA, 1984.
36. Rossa, J.; Villaverdeb, A.F.; Bangab, J.R.; Vazquezc, S.; Moranc, F. A generalized Fisher equation and its utility in chemical kinetics. *Proc. Natl. Acad. Sci. USA* **2010**, *107*, 12777–12781. [CrossRef] [PubMed]
37. Kerke, V.M. Results from variants of the Fisher equation in the study of epidemics and bacteria. *Physica A* **2004**, *342*, 242–248.
38. Merdan, M. Solutions of time-fractional reaction-diffusion equation with modified Riemann–Liouville derivative. *Int. J. Phys. Sci.* **2012**, *7*, 2317–2326. [CrossRef]
39. Stroud, K.A.; Booth, D.J. *Engineering Mathematics*; Bloomsbury Publishing: London, UK, 2020.
40. Brown, J.W.; Churchill, R.V. *Complex Variables and Applications*; McGraw-Hill: New York, NY, USA, 2009.
41. Guo, C.; Hu, J.; Wu, Y.; Celikovsky, S. Non-Singular Fixed-Time Tracking Control of Uncertain Nonlinear Pure-Feedback Systems With Practical State Constraints. *IEEE Trans. Circuits Syst. I Regul. Pap.* **2023**, *70*, 3746–3758. [CrossRef]
42. Li, D.; Ge, S.S.; Lee, T.H. Fixed-Time-Synchronized Consensus Control of Multiagent Systems. *IEEE Trans. Control Netw. Syst.* **2021**, *8*, 89–98. [CrossRef]
43. Shafee, A.; Alkhezi, Y.; Shah, R. Efficient Solution of Fractional System Partial Differential Equations Using Laplace Residual Power Series Method. *Fractal Fract.* **2023**, *7*, 429. [CrossRef]
44. Alkhezi, Y.; Shafee, A.; Shah, R. Fractional View Analysis of Partial Differential Equation via Residual Power Series Transform Method. *Appl. Math. Sci.* **2022**, *16*, 585–599. [CrossRef]
45. Alquran, M.; Ali, M.; Alsukhour, M.; Jaradat, I. Promoted residual power series technique with Laplace transform to solve some time-fractional problems arising in physics. *Results Phys.* **2020**, *19*, 103667. [CrossRef]
46. Alaroud, M. Application of Laplace residual power series method for approximate solutions of fractional IVP's. *Alex. Eng. J.* **2022**, *61*, 1585–1595. [CrossRef]
47. El-Tantawy, S.A.; Shah, R.; Alrowaily, A.W.; Shah, N.A.; Chung, J.D.; Ismaeel, S.M. A comparative study of the fractional-order Belousov—Zhabotinsky system. *Mathematics* **2023**, *11*, 1751. [CrossRef]
48. Bhalekar, S.; Daftardar-Gejji, V. New iterative method: Application to partial differential equations. *Appl. Math. Comput.* **2008**, *203*, 778–783. [CrossRef]
49. Zidan, A.M.; Khan, A.; Alaoui, M.K.; Weera, W. Evaluation of time-fractional Fishers equations with the help of analytical methods. *Aims Math* **2022**, *7*, 18746–18766. [CrossRef]
50. Falade, K.I.; Tiamiyu, A.T. Numerical solution of partial differential equations with fractional variable coefficients using new iterative method (NIM). *IJ Math. Sci. Comput.* **2020**, *3*, 12–21. [CrossRef]
51. El-Ajou, A. Adapting the Laplace transform to create solitary solutions for the nonlinear time-fractional dispersive PDEs via a new approach. *Eur. Phys. J. Plus* **2021**, *136*, 229. [CrossRef]
52. Daftardar-Gejji, V.; Jafari, H. An iterative method for solving nonlinear functional equations. *J. Math. Anal. Appl.* **2006**, *316*, 753–763. [CrossRef]
53. Bhalekar, S.; Daftardar-Gejji, V. Convergence of the new iterative method. *Int. J. Differ. Equ.* **2011**, *2011*, 989065. [CrossRef]
54. Botmart, T.; Alotaibi, B.M.; Shah, R.; El-Sherif, L.S.; El-Tantawy, S.A. A Reliable Way to Deal with the Coupled Fractional Korteweg-De Vries Equations within the Caputo Operator. *Symmetry* **2022**, *14*, 2452. [CrossRef]